AMR Seminar #75

Case – 1

Contributed by: Phil Allen, M.D.

Clinical History: A woman aged 42 presented with a history of a slowly growing, very large, protuberant tumor on the dorsum of her nose which blocked her nostrils and impeded her breathing. An initial core needle biopsy was suggestive of a perifollicular fibroma although clinically, the abnormality appeared to be a massive rhinophyma. The gross picture (below) shows the large, disfiguring, lobulated, asymmetric, exophytic mass with fissures completely covering the dorsum of the nose. Small pits, puncta or comedones are scattered across the surface of the rhinophyma and the skin of both cheeks. This disease has a rhinophyma severity index (RHISI) of 6, which is the maximum score.

The submitted specimen (below) consisted of a lobulated, fissured pedunculated mass measuring 65x45x40mm. The raw shave excision margin at the base, which measured 25x30mm, is visible at the lower part of the photograph beneath the suture.

Diagnosis: Giant rhinophyma.

The circulated sections show sebaceous hyperplasia, extensive keratotic plugging and dilatation of hair follicles with enlargement of the surface pores, intradermal budding of the basal cells, perifollicular chronic inflammatory cells, irregularly shaped, dilated, thin walled blood vessels and widespread interstitial fibrosis. No granulomas can be seen in most of the circulated slides but some non-caseating granulomas were found in other sections.

Comment: I had never previously seen sections of a giant rhinophyma so I thought that Club Members would like this case.

The clinical and histological features have recently been reviewed by Schuurmann and associates from Germany[(1)]. They believe that rhinophyma may occur de novo or as the final inflammatory phase of rosacea. It can be classified clinically into six grades of increasing severity using the rhinophyma severity index (RHISI), as proposed by Wetzig et al[(2)]. There is only mild skin thickening in grade 1, moderate skin thickening in grade 2, strong skin thickening and the formation of small lobules in grade 3, the additional presence of fissures in grade 4, the grossly enlarged deformity of a giant rhinophyma in grade 5, and marked asymmetry and multiple cysts, as in the current case, for grade 6. Lobules, fissures and the dilated pores of pilosebaceous openings are well shown in the asymmetrical exophytic enlargement of the nasal skin in the clinical picture above.

Most patients are males, which makes this case a little unusual. The grotesque, tumor-like component is confined to the nose but both cheeks are also involved by the disease. It is not clear why the exophytic growth affects the nose but not the cheeks. Perhaps it is due to the increased numbers of sebaceous glands located around the nose combined with the unyielding, underlying nasal cartilage which forces any enlargement to be exophytic, while on the cheek, there are only soft tissues beneath the expanding pilosebaceous units. The massive nasal enlargement is due to the combined effects of cystically dilated and keratin plugged hair follicles, sebaceous gland hyperplasia, vascular proliferation, chronic inflammation and interstitial fibrosis.

The clinical appearance of giant rhinophyma is so characteristic that a biopsy should not be necessary and may even be misleading, as in this case, where the core needle biopsy only included fibrous tissue and the edge of a hair follicle. In addition, the specimen was submitted without either an adequate description of the lesion or a clinical picture, which precluded a stand-alone histological diagnosis.

As opposed to rosacea, giant rhinophyma is comparatively rare but the grotesque appearance is likely to cause pity or even horror in observers, as happened in the case of J Pierpont Morgan (1837-1913), the founder of the financial institution J P Morgan and Co[(3)]. While J P Morgan with his deformity has been dead for over a hundred years, his name lives on in Australia as "Morgans Financial Limited."

The cause of the disease is unknown. Depending on its severity, rhinophyma can be treated with carbon dioxide laser or, as in this case, by shave excision and grafting. Recurrences are associated with a high pre-operative RHISI score[(1)].

References:

1. Schüürmann M, Wetzig T, Wickenhauser C, Ziepert M, Kreuz M, Ziemer M. Histopathology of rhinophyma - a clinical-histopathologic correlation. J Cutan Pathol. 2015; 42: 527-535.
2. Wetzig T, Averbeck M, Simon JC, Kendler M. New rhinophyma severity index and mid-term results following shave excision of rhinophyma. Dermatology 2013; 227: 31-36.
3. Dotz W, Berliner N. Rhinophyma. A master's depiction, a patron's affliction. Am J Dermatopathol 1984; 6: 231-235.

AMR Seminar #75

Case – 2

Contributed by: Kum Cooper, M.D.

Clinical History: Adult male with lung "tumor". Patient resides in Botswana.

Gross: Fragmented cystic lesion with surrounding lung tissue.

Microscopy: The cyst wall which appears in fragments in your slide comprise a diagnostic eosinophilic laminated wall with parts of the wall demonstrating a germinal layer.

Some slides may show a protoscolices which on high power show refractile hooklets.

Some slides show lung tissue with secondary granulomatous and chronic inflammation (and calcium).

Diagnosis: Hydatid cyst of the lung (Echinococcus granulosus) (Helminth, cestode).

Comment: The diagnosis is not difficult if you have encountered this characteristic laminated wall (cuticle) before.

This is a parasitic tapeworm with animals acting as the definitive host (commonly dogs and sheep in Southern Africa) with ingestion of contaminated water and food.

The swallowed eggs hatch in the small intestine and produce minute hooked embryos that burrow through the bowel and is transported to various organs such as the liver, lung, brain, eyes and bone.

The organisms produce a hydatid unilocular larval cyst (your slide) with an inner germinal layer that produces brood capsules which via an asexual budding process produces new larval tapeworms (protoscolices).

The cysts can achieve a large size from 2-30 cm with a thick wall and contain clear fluid (neutral pH, sodium chloride, proteins, glucose, ions, lipids and polysaccharides).

Needless to say, the fluid is antigenic and surgical removal is hazardous since rupture in the OR can result in anaphylactic shock.

AMR Seminar #75

Case – 3

Contributed by: Luca Di Tommaso, M.D., FIAC

Clinical History: A 59-year-old woman was seen for a persistent cough, not responsive to antibiotics. CT scans showed an 8 cm mass in the anterior mediastinum. She had no other significant history or evidence of tumor elsewhere. A biopsy was done, and the lesion diagnosed as a type A thymoma (p40+, PAX8+, Tdt+, CD5- e cKit-). A resection of the mass was undertaken. On cut section, the mass measured 8 cm. in greatest axis, showed well defined margins and was composed of whitish tissue admixed with haemorragic foci and areas of necrosis. The mass close to the resection margins.

Gross: Fragmented cystic lesion with surrounding lung tissue.

Pathological Findings: At histology the lesion was characterized by a dual component. The outer part was characterized by numerous, small clusters of p63+ neoplastic cells separated by lymphoid cells sometimes arranged in follicles. This part was consistent with a micronodular thymoma and observed only in few blocks. The outer part merged with the inner component which represented the majority of the tumor mass. This latter was made by p63+ neoplastic cells arranged in sheets and characterized by moderate/severe atypia, 1-5 mitosis/10 HPF and overt necrosis. Neoplastic cells stained positive for GLUT1 and negative for CD5 and c-kit. The lesion showed diffuse angioinvasion and capsule infiltration. Despite being close to a diagnosis of thymic carcinoma, the morphophenotypical findings were more consistent with an atypical type A thymoma.

Diagnosis: Atypical type A thymoma taking origin from a micronodular thymoma.

Comment: A possible relationship between type A thymoma and micronodular thymoma is illustrated and supported by data presented by the 2015 WHO. By contrast the relationship between atypical type A thymoma and micronodular thymoma is largely unknown. Accordingly, the case was sent to prof Suster and here are his comments:

"…I had never seen this before. I agree entirely with your interpretation of atypical spindle cell thymoma arising in a background of micronodular thymoma. The tumor is widely invasive into the capsule and there are some areas that could potentially represent vascular invasion; it might be worthwhile doing CD31 stains to evaluate those areas in the capsule. The areas with tumor necrosis are already bordering on thymic carcinoma, but the overall architecture is still that of an atypical thymoma. I would be very concerned for local recurrence and aggressive behavior."

AMR Seminar #75

Case – 4

Contributed by: **Barbara Gazic, M.D., PhD**

Clinical History: A 27-year-old female presented with a tumor of the uterine cervix.

Pathologic Features: The tumor measured 12x8.5 cm. It was multinodular, well circumscribed and protruded from the cervix into the vagina. On cut surface the tumor was lobulated and of soft consistency. Histologically the tumor is composed of spindle cells arranged in fascicular and focally also herringbone patterns. Brisk mitotic activity is present, and the tumor is focally necrotic. The tumor cells are strongly and diffusely positive for S100 and CD34 and negative for HMB45, Melanoma Cocktail, SMA, Desmin and CKAE1/AE3.

Based on morphology and immunohistochemistry the tumor was first diagnosed as malignant melanoma.

One year after surgery the tumor recurred in the soft tissue around the vaginal wall, the recurrence measured 3.5 centimeters in diameter. The patient was treated surgically again and also received radiotherapy in the area around vagina. She is in complete remission after the last treatment.

Because novel mesenchymal neoplasms of the uterus harboring recurrent translocations have recently been described, additional molecular testing was performed with NGS and EML4-NTRK3 fusion was confirmed.

Diagnosis: NTRK fusion positive uterine sarcoma.

Comment: NTRK-associated sarcomas of the uterine cervix usually arise in younger patients. Morphologically they resemble fibrosarcoma or MPNST. They are diffusely and strongly positive for CD34 and S100 and negative for desmin. Most of the rearrangements in NTRK-rearranged uterine sarcomas are TPM3-NTRK1 fusions and a minority are EML4-NTRK3 fusions. NTRK fusions are also consistently detected in congenital fibrosarcoma, congenital mesoblastic nephroma, secretory breast carcinoma and mammary analogue secretory carcinoma of the salivary gland as well as in some pediatric cancers but relatively rarely in lung cancer, colorectal cancer, papillary thyroid carcinoma, brain tumors, Spitzoid melanomas and adult soft tissue sarcomas. Identification of NTRK fusions is important because of the possibility of effective treatment with TRK inhibitors.

References:

1. Croce S, Hostein I, Longacre TA et al. Uterine and vaginal sarcomas resembling fibrosarcoma: a clinicopathological and molecular analysis of 13 cases showing common NTRK-rearrangements and the description of a COL1A1-PDGFB fusion novel to uterine neoplasms. Modern Pathology. 2019:1008-1022.
2. Gatalica Z, Xiu J, Swensen J, Vranic S. Molecular characterization of cancers with NTRK gene fusions. Modern Pathology. Published online 2018.

AMR Seminar #75

Case – 5

Contributed by: Ondřej Hes, M.D.

Clinical History: 73-year-old male was examined using ultrasonography during regular preventive check-up.

Exophytic renal tumor in pars intermedia of the left kidney was disclosed.

Laparoscopic resection of the tumor was indicated.

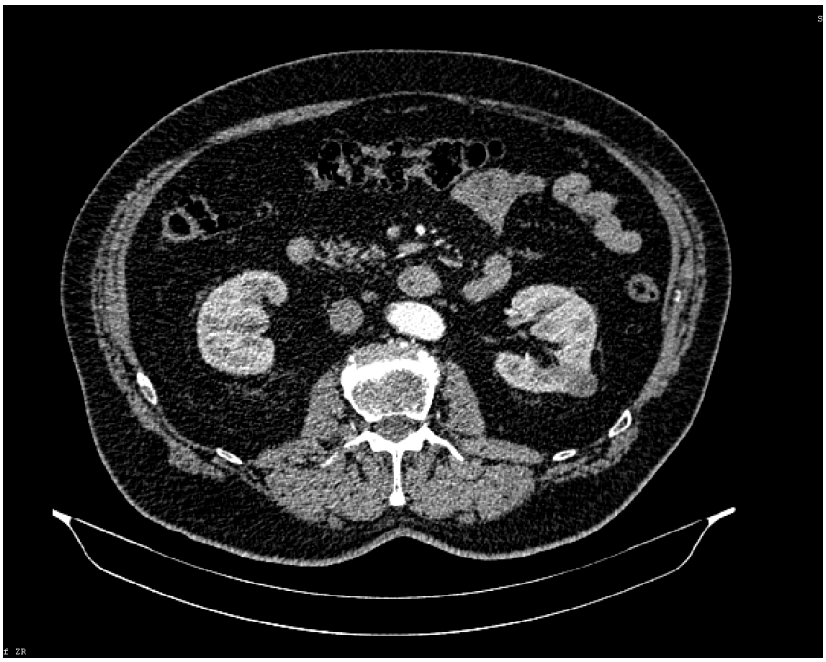

Well demarcated, non-capsulated very dark tumor was found, size 2.3 x 1.9 x 1.8 cm

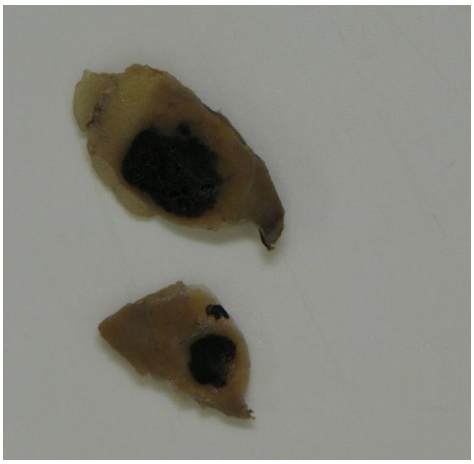

Histologic Findings: Tumor is composed of large cells growing in solid alveolar pattern. Stroma is edematous and hemorrhagic. Cells are pink with very prominent thick cell membranes, finely granular cytoplasm and large voluminous vacuoles. Nuclei are variable, round, irregular and/or wrinkled…occasionally with perinucleolar clearing.

Tumor was positive for AE1-AE3, CK8, CK 18, MIA, SDHB, and AMACR, focally positive for CK 7, cathepsin K, and cyclin D1. Tumor was negative for CD117, vimentin, Melan A, and HMB45.

Diagnosis: HOT (high grade oncocytic tumor)

Comment: High-grade oncocytic tumor (HOT) was recently described He et al. Authors reported multiinstitutional analysis of 14 cases. Subsequently, Chen et al reported a series of 7 morphologically identical tumors that they descriptively named as "sporadic renal cell carcinomas with eosinophilic and vacuolated cytoplasm". Case report referred novel case of HOT in a TSC patient showed an identical morphology and immunoprofile. Multiple concurrent tumors typically found in TSC patients were found in this particular patient. On the other hand, all patients from the He et al and Chen et al study, presented with solitary, tan-yellow to brown tumors, without any prior medical or family history of any syndromic disease (tuberous sclerosis particularly). All so far published tumors were stage pT1 (AJCC and UICC 2017). All patients reported in three studies (2 series and one case report) did not showed any aggressive clinical course. Median follow up was 12 and 28 months.

HOT demonstrate a relative uniform morphology and is composed of larger cells with eosinophilic granular cytoplasm with prominent cytoplasmic membranes. A significant component of the cells contain intracytoplasmic, voluminous vacuoles, resembling signet ring cell. A second cell component, often variable in size, demonstrates mostly pale (focally clear) cytoplasm. The nucleoli are enlarged and conspicuous (WHO/ISUP grade 3). Tumors have prominent thick-walled vessels at the periphery, as well as entrapped non-neoplastic tubules. Immunohistochemically, majority of cases are positive for CD117, negative or focally positive for CK7, and diffusely positive for MIA. Majority of tumors are positive with cathepsin K and CD10.

Molecular genetic testing was available for minor part of referred patients. Chen showed somatic inactivating mutations of *TSC2* or activating mutations of *MTOR*. Loss of chromosome 1 was found in cases with *MTOR* mutation; finding consistent with a hyperactive *MTOR* complex. He et al. showed changes in CNV pattern: losses of chromosome 1 (three of nine cases), chromosome19 (four of nine cases) and loss of heterozygosity on 16p11.2–11.1 (three of three cases) and 7q31.31 (two of three cases). No other chromosomal gains or losses were found.

Differential Diagnosis:
There are some rare renal tumors, which should be taken into the consideration in the differential diagnosis list. Translocation t6;11 renal cell carcinoma (TFEB) in it´s typical form is composed of large weakly eosinophilic cells with pseudorosettes surrounded by small epithelial lymphocyte-like cells. Tumor is immunoreactive for cathepsin K, HMB45 and/or Melan A. *TFEB* break is easily detectable using molecular genetic analysis.

SDH deficient RCC is another eosinophilic tumors composed of oncocytic elements with smaller intracytoplasmic vacuoles, entrapped thick walled vessels. Tumors are negative for SDHB with internal positive control. There are referred other patterns, however (and fortunately very rare).
Hybrid oncocytic/chromophobe renal cell carcinoma- they can be found in patients with Birt-Hogg-Dube (BHD) syndrome or within renal oncocytosis/oncocytomatosis or as sporadic cases. These tumors can be composed of areas similar to chromophobe RCC, to oncocytoma or they can share features of both. Such tumors miss huge intracytoplasmic vacuoles, thick walled entrapped vessels, and they usually do not have large irregular nuclei (or have raisinoid nuclei). In cases coming out of BHD syndrome, mutation of f*olliculin* gene should be found.

References:

1. He H, Trpkov K, Martinek P, Isikci OT, Maggi-Galuzzi C, Alaghehbandan R, Gill AJ, Tretiakova M, Lopez JI, Williamson SR, Perez Montiel D, Sperga M, Comperat E, Brimo F, Yilmaz A, Pivovarcikova K, Michalova K, Slouka D, Prochazkova K, Hora M, Bonert M, Michal M, Hes O.. "High-grade oncocytic renal tumor": Morphologic, immunohistochemical, and molecular genetic study of 14 cases. Virchows Arch 2018; 473; 725-738.
2. Chen YB, Mirsadraei L, Jayakumaran G, Al-Ahmadie HA, Fine SW, Gopalan A, Sirintrapun SJ, Tickoo SK, Reuter VE. Somatic mutations of tsc2 or mtor characterize a morphologically distinct subset of sporadic renal cell carcinoma with eosinophilic and vacuolated cytoplasm. Am J Surg Pathol 2019; 43; 121-131.
3. Trpkov K, Bonert M, Gao Y, Kapoor A, He H, Yilmaz A, Gill AJ, Williamson SR, Comperat E, Tretiakova M, Magi-Galluzzi C, Brimo F, Hes O. High-grade oncocytic tumour (HOT) of kidney in a patient with tuberous sclerosis complex.
Histopathology. 2019 Apr 19. In press

AMR Seminar #75

Case – 6

Contributed by: Jesse McKenney, M.D.

Clinical History: A 61-year-old man presented with gross hematuria and was subsequently found to have a 5 cm right renal mass and retroperitoneal adenopathy. He underwent a radical nephrectomy, which showed the neoplasm represented by the enclosed slide.

Diagnosis: Metastatic adenocarcinoma of lung origin (with micropapillary features) presenting as primary renal mass

Comment: By immunohistochemistry, the carcinoma had strong and diffuse nuclear TTF-1 reactivity, while PAX8, p63, HMWCK, and GATA3 were all negative. FH (Fumarate Hydratase) showed retained cytoplasmic staining and nuclear INI-1 expression was also retained. After a pathologic diagnosis of "adenocarcinoma suspicious for metastasis from lung origin" was rendered, a chest CT showed a 1.2 cm spiculated lesion consistent with a primary lung cancer. The patient has subsequently developed liver and adrenal metastases.

I included this case because of the differential diagnostic discussion it elicited for high grade carcinomas of the kidney with destructive invasion: collecting duct carcinoma, medullary carcinoma, FH deficient RCC, urothelial carcinoma with glandular differentiation, and metastatic adenocarcinoma. I have yet to personally see a convincing case of "collecting duct carcinoma" despite our very large renal tumor volume. On review of the surgical pathology archives at CCF by our GU section, we think that many cases historically diagnosed as "collecting duct" would now be regarded as urothelial carcinomas with glandular differentiation (with modern immunohistochemical markers) or FH deficient RCC (RCC associated with Hereditary Leiomyomatosis and Renal Cell Carcinoma syndrome- HLRCC). This is in keeping with the observations of many other authors. We regard "collecting duct carcinoma" as a diagnosis of absolute exclusion, such that it seems to be extraordinarily rare (at best) if appropriate differential diagnostic possibilities are excluded.

AMR Seminar #75

Case – 7

Contributed by: **Markku Miettinen, M.D.**

Clinical history: 49-year-old female 20x10x10 cm upper abdominal soft tissue mass. Grossly myxoid, focally rubbery.

Diagnosis: GIST with a histological imatinib response.

Comment: Imatinib-treated GISTs are seen in an increasing frequency because imatinib is often used in neoadjuvant capacity, i.e. before definitive surgery takes place. A typical histological response includes the following features: Loss of cellularity, increased myxoid matrix, and shrunken residual tumor cells. All these features are seen in the current case. Return of islands of cells with pre-treatment appearance may indicate a secondary mutation that escapes imatinib treatment (KIT exon 13, exon 14, or exon 17 mutations).

AMR Seminar #75

Case – 8

Contributed by: Fredrik Petersson, M.D.

Clinical History and Gross Features: The patient is a 48-year-old man with diabetes mellitus. He presented with intermittent and both anterior and posterior and anosmia for 1 year and 2 months, respectively. An MRI scan of the nasal cavity and sinuses showed a 6.5 cm, heterogeneously enhancing mass centered in the right nasal cavity, eroding the wall of the right maxillary sinus with extension into the nasopharynx and bilateral ethmoid air cells.

Histology: An initial biopsy showed a cellular tumour in the subepithelial stroma extending close to the respiratory tract mucosal surface. The tumour was composed of sheets of monomorphic cells with round to ovoid nuclei, small amounts of pale cytoplasm and indistinct cytoplasmic boundaries. The chromatin was evenly distributed with occasional intra-nuclear vesicles and small nucleoli. Mitotic activity was low. Aggregates of osteoclast-like giant cells were present, along with small areas of "smudgy", basophilic stroma with a tendency to form chicken-wire type calcifications. There was no evidence of high-grade cytological atypia or necrosis.

Immunohistochemistry: The tumour cells exhibited no immunohistochemically detectable expression of smooth muscle actin (SMA), CD34, desmin, S-100 protein or cytokeratins (AE1/3).

Diagnosis and Comments: The diagnosis is ***phosphaturic mesenchymal tumour***.

After the possibility of PMT was raised in the initial biopsy report, further clinical information was gathered, and the patient responded positively to having experienced bone pain. Subsequent laboratory investigations revealed hypophosphatemia (0.46 mmol/L, N = 0.85 - 1.45), low-normal serum calcium (2.18 mmol/L, N = 2.15 - 2.55), and insufficient 25-OH Vitamin D levels (24 µg/L, sufficient > 29). The biochemical findings were consistent with those of oncogenic osteomalacia (OO) and the patient subsequently underwent endoscopic, piecemeal resection of the sinonasal tumour. Additional histological features seen in the resection specimen include microcyst formation and of mature adipocytes. In some areas, the cells exhibited a more rounded morphology, and the microvasculature featured thin-walled, capillaries surrounded by myxoid, hypocellular tumour containing spindled to stellate tumour cells. The tumour was positive for FGF-23 expression by chromogenic in situ hybridization tumour cells also exhibited cytoplasmic/membranous fibroblast growth factor receptor 1 (FGFR1) protein expression by immunohistochemistry which was not observed in the osteoclast-like giant. 19 days postoperatively, the serum calcium and phosphate levels were normalized (S-Ca 2.11, S-P 1.25). The patient has remained disease-free with no evidence of recurrence during a follow-up period of >5 years.

Phosphaturic mesenchymal tumour (PMT) denotes a rare neoplastic entity that is the most common cause of the paraneoplastic syndrome oncogenic osteomalacia (1,2). In 2004, Folpe et. al provided corroborative evidence for PMT being a histologically distinct entity encompassing a characteristic set of morphological features in varying proportions. These include the presence of bland ovoid to spindled cells, cartilage-like matrix, osteoclast-like giant cells, microcysts, prominent blood vessels, and metaplastic bone (2). PMT occurs mostly in middle-aged adults with no apparent gender predilection (2). It occurs most commonly in the lower extremities less frequently in the head and neck region including the sinonasal tract, and rarely, in locations such as the skin, meninges, thyroid and mediastinum (9-14).

The clinical manifestations are highly variable, and the differential diagnoses to be considered are influenced by the location of the presenting tumour. Although PMT is the most common cause of OO, it is not the only cause, warranting histological confirmation of the neoplasm. Whilst PMT exhibits distinctive histological characteristics, ancillary tests have played a role in the characterisation of this tumour. The best studied marker expressed by most PMTs is FGF-23, a protein that regulates phosphate reabsorption in the renal proximal tubules (2). Serum FGF-23 levels, on the other

hand, may be within normal limits even with clinical evidence of OO (15), suggesting the role of other hormones in the pathophysiology of OO associated with PMT. A few studies have also described the strong and diffuse expression of somatostatin receptor 2A (SSTR2A) detected by immunohistochemistry in PMT; however, neither FGF-23 nor SSTR2A are specific for PMT, as they are expressed in other mesenchymal tumours (14-16). More recently, a novel FN1-FGFR1 genetic fusion has been described in nine out of 15 (60%) of PMTs (5). FGFR1 is a member of the fibroblast growth factor receptor (FGFR) family of receptor tyrosine kinases that has been implicated in the tumourigenesis of a wide range of solid tumours and haemopoietic malignancies (17,19). The predicted consequences of the FN1-FGFR1 gene fusion include overexpression of a chimeric FGFR1 with preserved ligand binding properties under the control of the fibronectin (FN1) promoter, that may provide an advantage of elevated concentrations of its ligands (such as FGF23) in promoting tumourigenesis via receptor tyrosine-kinase activation (5). PMT is deemed to be a predominantly benign lesion, although reports of malignant variants have been reported (20-22).

Histological features of malignancy in PMT include areas of high nuclear grade, high cellularity, and elevated mitotic activity (2). Of interest, histological evidence of dedifferentiation and malignant transformation over multiple recurrences has been reported (23), illustrating the importance of thorough histological sampling in the context of recurrent disease.

Figures

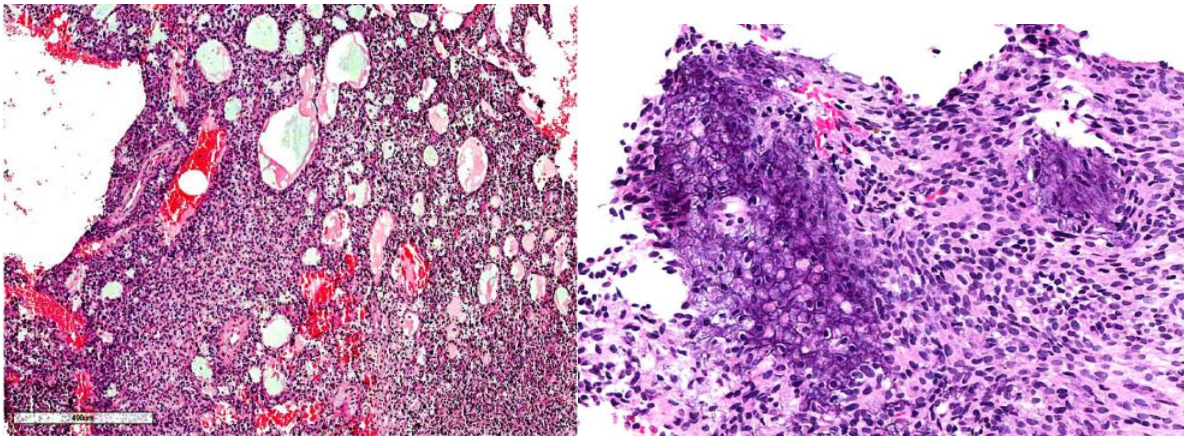

References:

1. Weidner N, Santa Cruz D. Phosphaturic mesenchymal tumors. A polymorphous group causing osteomalacia or rickets. Cancer 1987;59;1442-1454.
2. Folpe AL, Fanburg-Smith JC, Billings SD et al. Most osteomalacia-associated mesenchymal tumors are a single histopathologic entity: An analysis of 32 cases and a comprehensive review of the literature. Am J Surg Pathol 2004;28;1-30.
3. Consortium A. Autosomal dominant hypophosphataemic rickets is associated with mutations in fgf23. Nat Genet 2000;26;345-348.
4. Liu S, Gupta A, Quarles LD. Emerging role of fibroblast growth factor 23 in a bone-kidney axis regulating systemic phosphate homeostasis and extracellular matrix mineralization. Curr Opin Nephrol Hypertens 2007;16;329-335

5. Lee JC, Jeng YM, Su SY et al. Identification of a novel fn1-fgfr1 genetic fusion as a frequent event in phosphaturic mesenchymal tumour. J Pathol 2015;235;539-545.

6. Carter JM, Caron BL, Dogan A, Folpe AL. A novel chromogenic in situ hybridization assay for fgf23 mrna in phosphaturic mesenchymal tumors. Am J Surg Pathol 2015;39;75-83.

7. Peterson NR, Summerlin DJ, Cordes SR. Multiple phosphaturic mesenchymal tumors associated with oncogenic osteomalacia: Case report and review of the literature. Ear Nose Throat J 2010;89;E11-15.
8. Shelekhova KV, Kazakov DV, Michal M. Sinonasal phosphaturic mesenchymal tumor (mixed connective tissue variant): Report of 2 cases. Am J Surg Pathol 2010;34;596-597.
9. Gardner KH, Shon W, Folpe AL, Wieland CN, Tebben PJ, Baum CL. Tumor-induced osteomalacia resulting from primary cutaneous phosphaturic mesenchymal tumor: A case and review of the medical literature. J Cutan Pathol 2013;40;780-784; quiz 779.
10. Mathis DA, Stehel EJ, Jr., Beshay JE, Mickey BE, Folpe AL, Raisanen J. Intracranial phosphaturic mesenchymal tumors: Report of 2 cases. J Neurosurg 2013;118;903-907.
11. Harvey JN, Gray C, Belchetz PE. Oncogenous osteomalacia and malignancy. Clin Endocrinol (Oxf) 1992;37;379-382.
12. Tsujimura T, Sakaguchi K, Aozasa K. Phosphaturic mesenchymal tumor, mixed connective tissue variant (oncogenic osteomalacia). Pathol Int 1996;46;238-241.
13. Kumar R. New insights into phosphate homeostasis: Fibroblast growth factor 23 and frizzled-related protein-4 are phosphaturic factors derived from tumors associated with osteomalacia. Curr Opin Nephrol Hypertens 2002;11;547-553.
14. Clugston E, Gill AC, Graf N, Bonar F, Gill AJ. Use of immunohistochemistry for sstr2a to support a diagnosis of phosphaturic mesenchymal tumour. Pathology 2015;47;173-175.
15. Graham R, Krishnamurthy S, Oliveira A, Inwards C, Folpe AL. Frequent expression of fibroblast growth factor-23 (fgf23) mrna in aneurysmal bone cysts and chondromyxoid fibromas. J Clin Pathol 2012;65;907-909.
16. Houang M, Clarkson A, Sioson L et al. Phosphaturic mesenchymal tumors show positive staining for somatostatin receptor 2a (sstr2a). Hum Pathol 2013;44;2711-2718.
17. Dienstmann R, Rodon J, Prat A et al. Genomic aberrations in the fgfr pathway: Opportunities for targeted therapies in solid tumors. Ann Oncol 2014;25;552-563.
18. Xiao S, Nalabolu SR, Aster JC et al. Fgfr1 is fused with a novel zinc-finger gene, znf198, in the t(8;13) leukaemia/lymphoma syndrome. Nat Genet 1998;18;84-87.
19. Graham RP, Hodge JC, Folpe AL et al. A cytogenetic analysis of 2 cases of phosphaturic mesenchymal tumor of mixed connective tissue type. Hum Pathol 2012;43;1334-1338.
20. Sidell D, Lai C, Bhuta S, Barnes L, Chhetri DK. Malignant phosphaturic mesenchymal tumor of the larynx. Laryngoscope 2011;121;1860-1863.
21. Uchihashi K, Nishijima-Matsunobu A, Matsuyama A et al. Phosphaturic mesenchymal tumor, nonphosphaturic variant, causing fatal pulmonary metastasis. Hum Pathol 2013;44;2614-2618.
22. Uramoto N, Furukawa M, Yoshizaki T. Malignant phosphaturic mesenchymal tumor, mixed connective tissue variant of the tongue. Auris Nasus Larynx 2009;36;104-105.
23. Ogose A, Hotta T, Emura I et al. Recurrent malignant variant of phosphaturic mesenchymal tumor with oncogenic osteomalacia. Skeletal Radiol 2001;30;99-103.

AMR Seminar #75

Case – 9

Contributed by: Santiago Ramon y Cajal, M.D.

Clinical history: A 4-year-old male detected an intraocular tumor. The eye and 0.3cm of optic nerve are removed. Externally no changes are observed. In its opening a whitish, granular and dense tumor mass is observed that occupies 70% of the vitreous with a 4cm diameter base that displaces the retina. Apparent macroscopic involvement of the macular area and optic nerve.

Microscopic Description and Diagnosis: The tumor shows blastic characteristics with a high mitotic index, small foci of necrosis and occasional rosettes.

Diagnosis: Undifferentiated retinoblastoma of exophytic predominance with mild necrosis (less than 10%) and high mitotic index.

Comment: I send this case, given the rarity of retinoblastomas in surgical specimens. Retinoblastomas are unusual tumors with an incidence less than one case for every 20,000 children born alive. They are much more frequent in children under 3 years old and currently the cure rate is >90-95% of cases.

Clinically it is usually detected by alterations at the level of the pupil, which parents usually identify as, changes in color or leukocoria that reflect an intraocular lesion.

The tumors are blastic in appearance with different degrees of differentiation. In some, the rossetes are of the Flexner type, which shows cuboidal cells that circumscribe the light. In more differentiated cases the Homer Wright rosettes, similar to neuroblastic tumors where the cells are not arranged around a lumen, but the central core is occupied by cytoplasmic processes thereof.

The treatment has evolved from surgery, radiotherapy to chemotherapy treatments. Nowadays are mostly based more on local chemotherapy treatment.

AMR Seminar #75

Case – 10

Contributed by: Murray Resnick, M.D.

Clinical History: This slide comes from a right colectomy of an 80-year-old female. The right colon cancer had loss of MMR proteins by IHC and exhibited a BRAF mutation consistent with sporadic MSI. Morphologically the tumor had mucinous features (as well as signet ring features best seen in other slides) in keeping with an MSI-H tumor.

Immunohistochemical Findings: The pathologist who reviewed this case noticed a serosal/subserosal area of adenocarcinoma which looked morphologically distinct from the adjacent colonic adenocarcinoma. Although different patterns of adenocarcinoma are not uncommon in MSI tumors the pathologist felt it was best to work this area up by IHC. As can be seen in the attached figures the subserosal focus was TTF+/CDX2- as opposed to the adjacent tumor which was TTF-/CDX2+. Of course, the fact that the patient had a history of lung adenocarcinoma (and RCC for that matter) was not stated in the requisition and only on further digging in EPIC was this history obtained. Further examination of the gross specimen revealed additional serosal deposits on the surface of the colon and appendix.

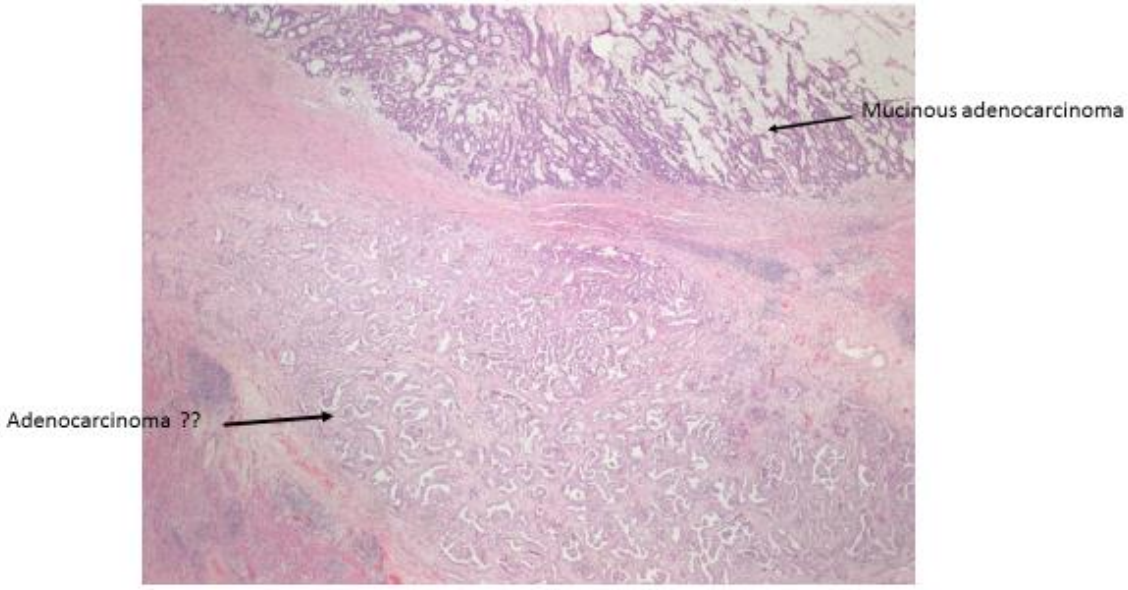

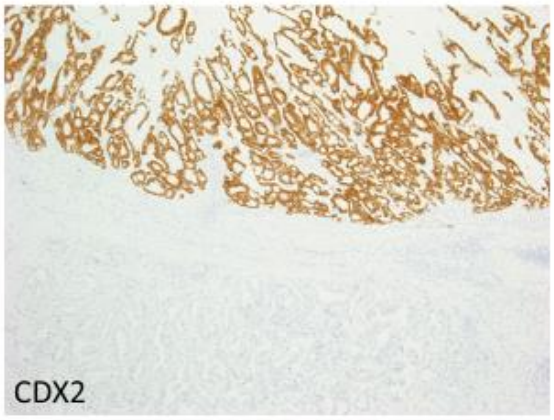

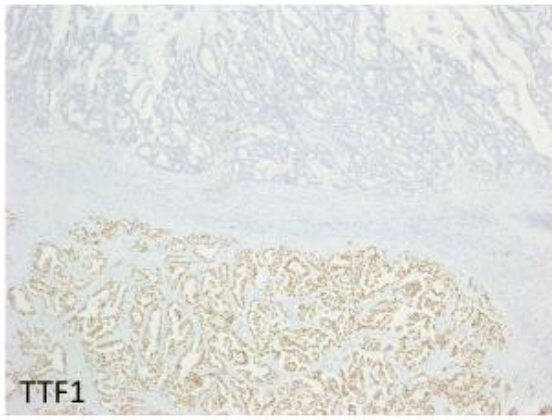

Diagnosis: Lung cancer metastatic to the GI tract

Comment: Lung cancer metastatic to the GI tract is relatively rare. Autopsy studies have demonstrated GI involvement in 0.2% to 11.9% of all cases whereas only 0.2%-0.5% of lung cancer patients had symptomatic involvement of the GI tract. The most common site of involvement is the small bowel, and squamous and small cell carcinomas more commonly metastasize than adenocarcinomas.

All of the studies discuss luminal involvement of the GI tract as opposed to the serosal involvement seen here. I could not easily find reports of lung cancer metastatic to regions involved by colon cancer.

References:

1. Yang CJ, Hwang JJ, Kang WY, Chong IW, Wang TH, Sheu CC, Tsai JR, Huang MS: Gastro-intestinal metastasis of primary lung carcinoma: clinical presentations and outcome. Lung Cancer. 2006, 54 (3): 319-323. 10.1016/j.lungcan.2006.08.007
2. Yoshimoto A, Kasahara K, Kawashima A: Gastrointestinal metastases from primary lung cancer. Eur J Cancer. 2006, 42 (18): 3157-3160. 10.1016/j.ejca.2006.08.030.

AMR Seminar #75

Case – 11

Contributed by: Kenneth Schoolmeester, M.D.

Clinical History: A 27-year-old woman recently underwent evacuation of a complete hydatidiform mole. Two weeks later, the patient had persistently elevated beta-hCG and underwent endometrial curettage.

Microscopic Findings: Sections show a proliferation of hyperchromatic and pleomorphic implantation site intermediate trophoblast aggregates and involving endometrium. No other types of trophoblast are present.

Diagnosis: Molar-associated exaggerated placental/implantation site.

Comment: Molar-associated exaggerated placental/implantation sites are an underappreciated phenomenon that frequently occurs in complete hydatidiform moles. They're differentiated from typical or non-molar exaggerated placental/implantation sites by marked hyperchromasia and nuclear pleomorphism or enlargement. This degree of nuclear atypia in implantation site intermediate trophoblast is essentially diagnostic of either concurrent or recent molar gestation.

References:

1. Montes M et al. Prevalence and significance of implantation site trophoblastic atypia in hydatidiform moles and spontaneous abortions. Am J Clin Pathol. 1996;105:411-6.

AMR Seminar #75

Case – 12

Contributed by: Ady Yosepovich, M.D.

I want to thank Dr. Ira Bleiweiss, my mentor and friend for his help with this case.

Clinical History: This is a 46-year-old lady with family history of breast ca+colon (mother). And colon + lung ca (father) – genetics- not clear.

She noticed a left breast mass.

Mammography showed a well circumscribed mass in the upper-outer quadrant 2. 8

CM in major diameter. BIRADS 4B.

US showed a well circumscribed heterogenic mass.

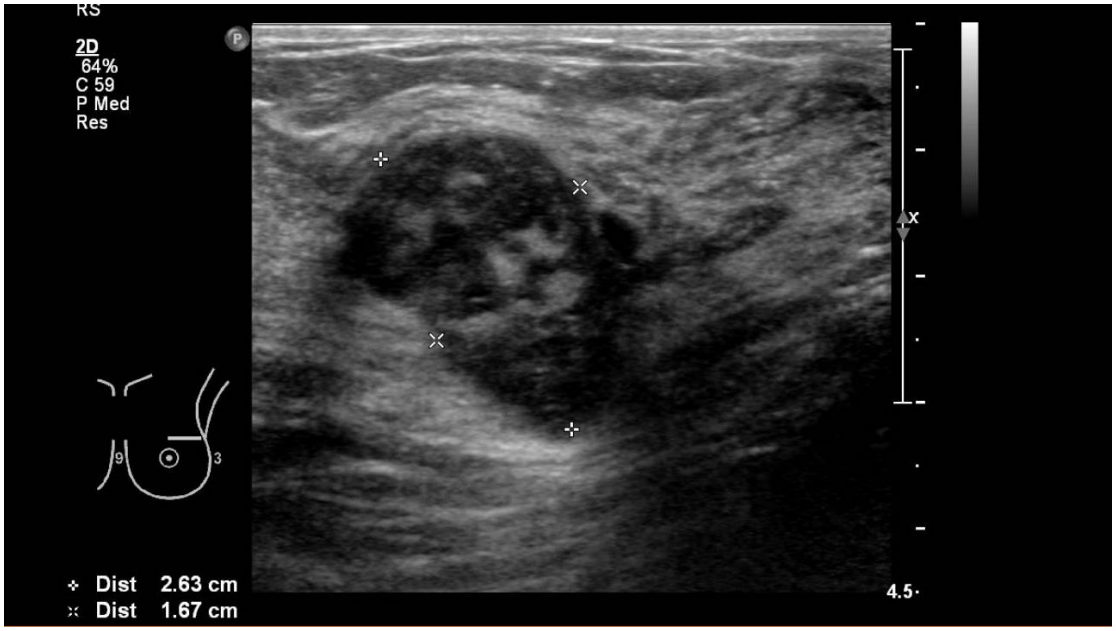

CNB was performed – suspicious for phylodes tumor.

Lumpectomy was performed.

Histological Findings: On histological evaluation a fibro-epithelial lesion is recognized with lobulated non-homogenic areas. At areas, the stroma shows severe hypercelularity, atypia of the cells with mitotic activity. Mixoid material is noticed with "chicken wire" vessels. Lipoblasts are identified with scalloped nuclei and cytoplasmic vacuoles.

The ducts show proliferating epithelial cells, cribriform architecture is present. Comedo-nerosis is present. Moderate to high grade nuclear atypia is observed. The atypical cells spread in a pagetoid pattern to ducts outside the lesion.

Diagnosis: Malignant Phylodes tumor with Myxoid liposarcomatous elements associated with Intermediate to High Grade Duct Carcinoma in Situ.

Comment: Your slide is from the lumpectomy specimen; I am not sure that all slides contain all features, so I added some pictures.

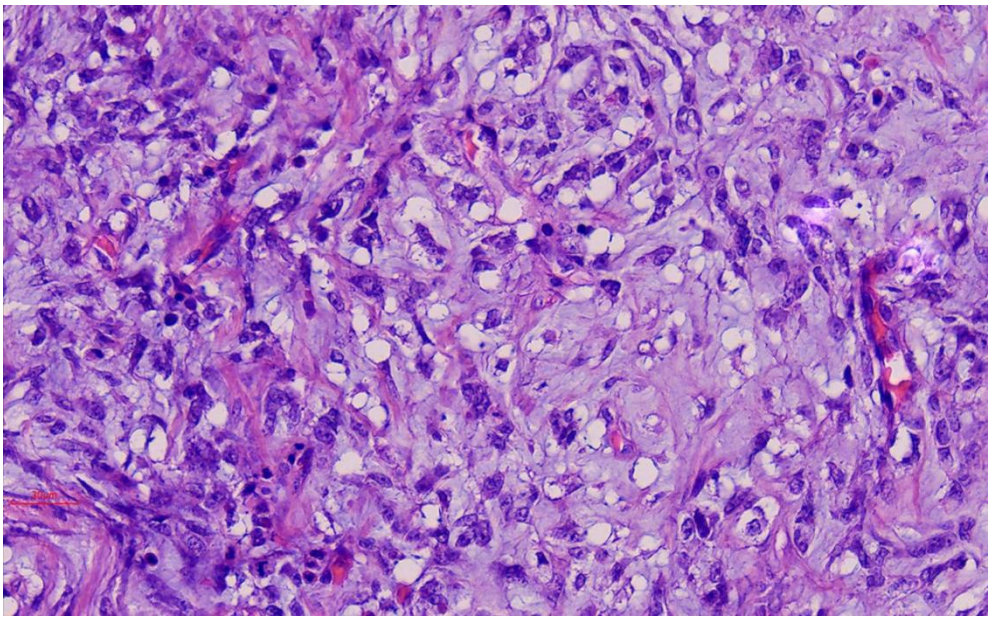

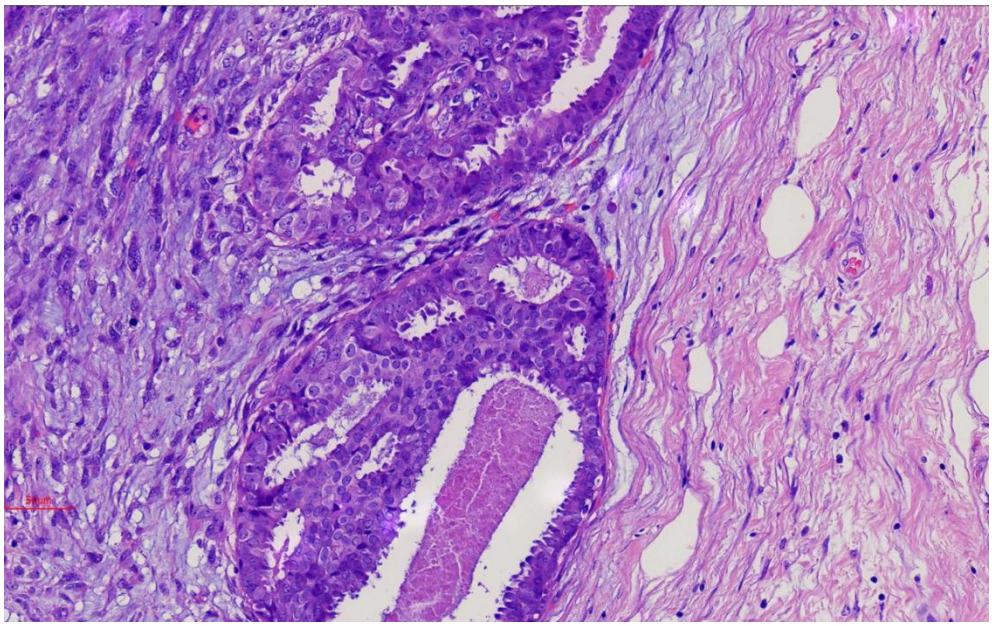

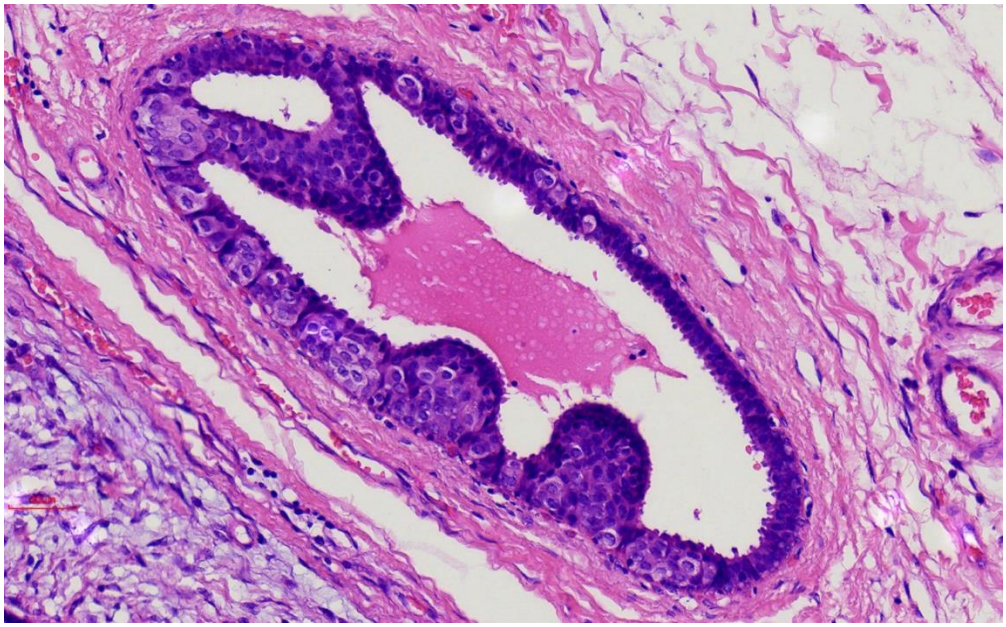

AMR Seminar #75

Case – 13

Contributed by: Cyril Fisher, M.D.

Clinical History: A 51-year-old female had an RLQ breast mass. A core needle biopsy showed sheets of focally vacuolated diagnosed as triple negative primary carcinoma. The patient was treated with chemotherapy but the tumor progressed and mastectomy was performed. Both slides are from the latter (slide A has appearances as in the core biopsy).

Macroscopic appearances: The breast contained a well-defined tumour 5cm in diameter with yellow, white and gelatinous areas.

Micropscpic appearances: Slide A shows the features seen on the core biopsy, of a neoplasm composed of sheets of polygonal cells with rounded nuclei, clear cytoplasm and distinct cell boundaries. There is focal pleomorphism and mitotic activity. No in situ component is seen in the adjacent breast tissue. Immunohistochemistry on the core biopsy was focally positive for MNF116 (but not other cytokeratins or EMA), E-cadherin, GATA3, and S100 protein. ER, PgR and Her2 were negative.

Slide B shows areas of similar tumour and larger foci comprising markedly pleomorphic spindle and polygonal cells with mitoses, tumour giant cells, and multivacuolated lipoblast-like cells. There are also foci of necrosis. Immunohistochemistry is focally positive for S100 protein and negative for cytokeratins, E-cadherin, ER, PgR, GCDFP15 and GATA3. Other negative markers include desmin, CD34, p63, melan-A, HMB45. FISH studies for MDM2 amplification and DDIT3 (CHOP) gene rearrangement were negative.

Diagnosis: Epithelioid variant of pleomorphic liposarcoma.

Comment: This is an epithelioid-looking neoplasm focally expressing mainly cytokeratin and S100 protein, merging into areas of typical pleomorphic liposarcoma. Epithelioid pleomorphic liposarcoma is a relatively rare entity, with one initial series[1] followed by case reports in soft tissue and mediastinum[2]. A resemblance to adrenal cortical carcinoma has been noted in some examples. Among published series of pleomorphic liposarcoma, 7 of 19 cases[3], 6 of 40 cases [4] and 4 of 32 cases[5] were predominantly epithelioid. However, only rare examples have been reported arising in the breast parenchyma and in the overlying subcutis.[5] Focal cytokeratin and S100 protein positivity are typical. *FUS-CHOP* transcripts, as usually seen in myxoid liposarcoma, have been described in a single case report (albeit with images more suggestive of round cell liposarcoma).[6] The absence of MDM2 amplification also excludes dedifferentiated liposarcoma with homologous lipoblastic differentiation.

In this location the differential diagnosis includes pleomorphic liposarcoma arising in metaplastic carcinoma, of which only very few cases have been described.[7] This case had focal cytokeratin positivity but it does not resemble the usual breast carcinoma, no in situ component was found, no other sarcomatous elements are seen and there was no response to chemotherapy. Pleomorphic liposarcoma can also rarely arise in malignant phyllodes tumour, of which no features are seen here.[8]

References:

1. Miettinen M, Enzinger FM. Epithelioid variant of pleomorphic liposarcoma: a study of 12 cases of a distinctive variant of high-grade liposarcoma. Mod Pathol. 1999;12:722-728.

2. Boland JM, Colby TV, Folpe AL. Liposarcomas of the mediastinum and thorax: a clinicopathologic and molecular cytogenetic study of 24 cases, emphasizing unusual and diverse histologic features. Am J Surg Pathol. 2012;36:1395-1403.

3. Downes KA, Goldblum JR, Montgomery EA, Fisher C. Pleomorphic liposarcoma: a clinicopathologic analysis of 19 cases. Mod Pathol. 2001;14:179-84.

4. Ghadimi MP, Liu P, Peng T, Bolshakov S, Young ED, Torres KE, Colombo C, Hoffman A, Broccoli D, Hornick JL, Lazar AJ, Pisters P, Pollock RE, Lev D. Pleomorphic liposarcoma: clinical observations and molecular variables. Cancer 2011;117:5359-5369.

5. Wang L, Ren W, Zhou X, Sheng W, Wang J. Pleomorphic liposarcoma: a clinicopathological, immunohistochemical and molecular cytogenetic study of 32 additional cases. Pathol Int. 2013;63:523-531.

6. De Cecco L, Gariboldi M, Reid JF, Lagonigro MS, Tamborini E, Albertini V, Staurengo S, Pilotti S, Pierotti MA. Gene expression profile identifies a rare epithelioid variant case of pleomorphic liposarcoma carrying FUS-CHOP transcript. Histopathology. 2005;46:334-341

7. Elghobashy M, Basu N, Warner R, Dickson J, Shaaban AM. Metaplastic breast cancer masquerading as liposarcoma of the breast: a case report following oncoplastic treatment. Pathobiology. 2018;85:261-265.

8. Bacchi CE, Wludarski SC, Lamovec J, Ben Dor D, Ober E, Salviato T, Zanconati F, De Maglio G, Pizzolitto S, Sioletic S, Falconieri G. Lipophyllodes of the breast. A reappraisal of fat-rich tumors of the breast based on 22 cases integrated by immunohistochemical study, molecular pathology insights, and clinical follow-up. Ann Diagn Pathol. 2016;21:1-6

AMR Seminar #75
Case – 14

Contributed by: Kyle Perry, M.D.

Clinical History: The patient is a 73-year-old male who presented with groin pain and was found on plain films/CT scan to have a chondral lesion in the right femoral intertrochanteric region. MRI showed T2 hyperintensity consistent with a chondroid neoplasm. Interestingly, the patient has a smaller lesion with likely chondroid features on the contralateral femur.

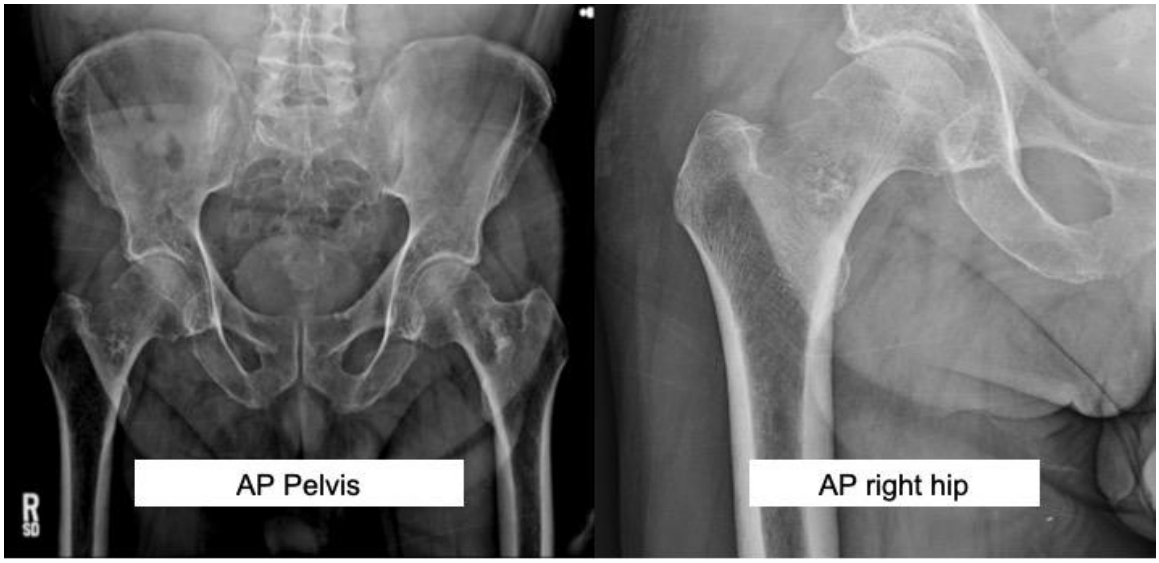

3

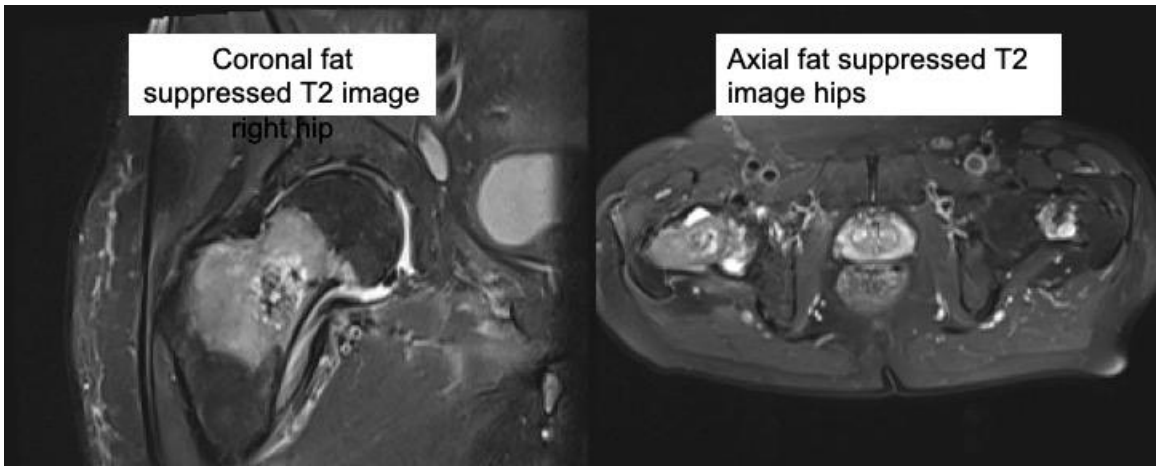

A CT-guided biopsy showed a proliferation of spindled cells with only mild nuclear atypia (see Fig 1a). High grade sarcomatous morphology was not identified. Given the disparity of these findings with the radiologic presentation, an open biopsy was performed. The open biopsy showed substantial areas of cellular necrosis with scattered spindled cells with relatively limited nuclear atypia (Fig 1b and 1c). Fragments of hyaline cartilage were also seen (Fig 1d). Of note, the open biopsy is the slide which I included.

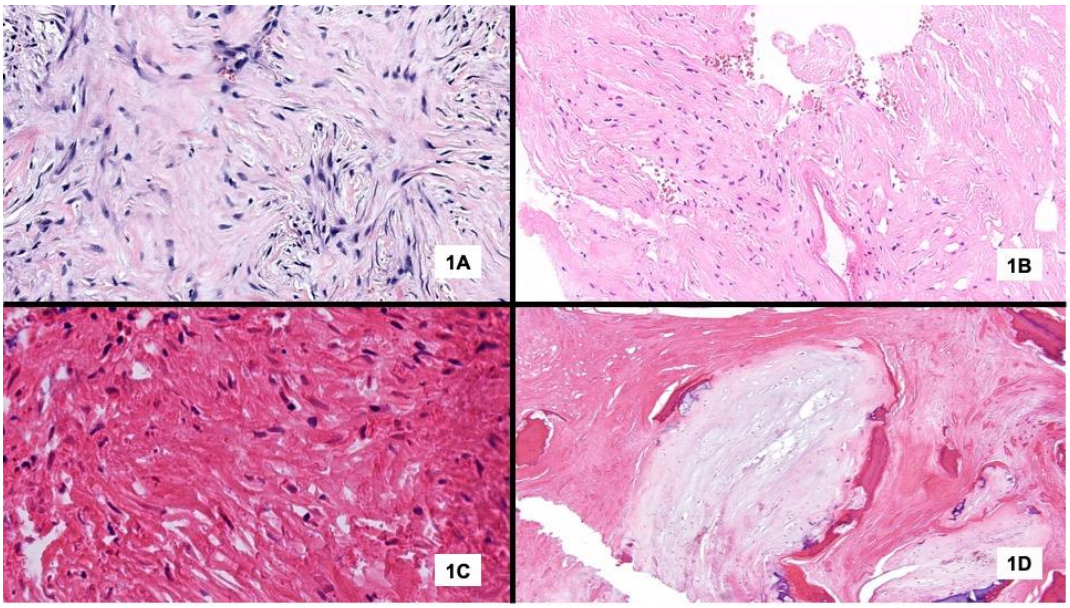

Following the open biopsy, the tumor was then resected. A substantial portion of the tumor showed a spindle cell proliferation with similar features (Fig 2a); however, these spindled cells appeared to show a more permeative architecture (Fig 2b). Scattered areas with increased nuclear atypia were also identified (Fig 2c).

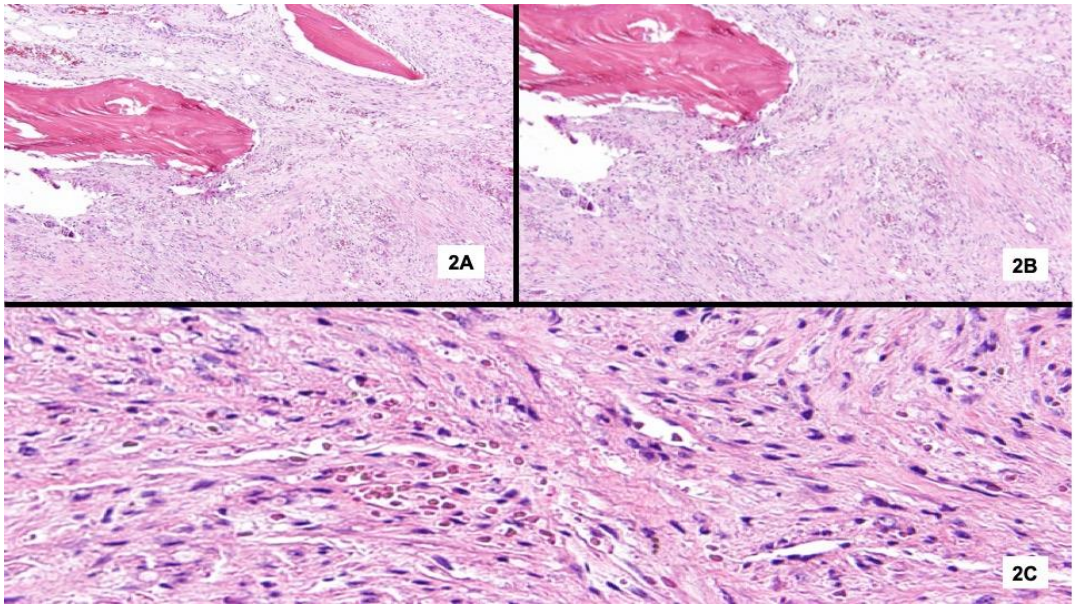

Diagnosis: Dedifferentiated chondrosarcoma (with mild to moderate nuclear atypia), likely arising from an enchondroma.

Comment: Although dedifferentiated chondrosarcoma is not a particularly exotic entity, I thought some might find this particular presentation of interest.

Dedifferentiated chondrosarcoma is typically characterized by a low-grade cartilaginous lesion (often resembling a grade 1 chondrosarcoma) that abruptly transitions to an unequivocal high-grade sarcoma. The high-grade sarcoma component can contain areas of heterologous differentiation (e.g. rhabdomyosarcoma, osteosarcoma).

In this case, there was not an extensive viable high-grade sarcoma component. Many of the viable spindled cells contains nuclei with mild to focally moderate atypia. Within the confines of the needle core biopsy material, I found it difficult to commit to a definitive classification of sarcoma.

We sent the needle core and open biopsy to Dr. Andrew Rosenberg, who felt that the overall features (in conjunction with the imaging findings) would be diagnostic of a dedifferentiated chondrosarcoma. Additionally, we performed Sanger Sequencing on the spindle cells in the core biopsy which revealed an IDH2 mutation, consistent (in the context of morphology/imaging) with a dedifferentiated chondrosarcoma (1).

While dedifferentiation of chondrosarcomas and liposarcomas typically occurs as a defined and abrupt transition between low and high-grade morphologies, variant patterns can prove more difficult when sampled by needle core biopsy. These tumors can occasionally have a mosaic pattern in which the high-grade component is present in only multiple microscopic foci(2). In this particular case, the lack of a substantial high-grade viable component personally caused some difficulty for me. In Dorfman and Czerniak's Bone Tumors, the authors note that incidences of a "low-grade fibroblastic osteosarcoma or fibrosarcoma are extremely rare."(3) Given the substantial coagulative necrosis in our particular case, it is strongly possible that there could have been a more apparent high-grade morphologic component that underwent necrosis prior to biopsy and resection.

After resection, follow-up imaging revealed the patient to likely have two areas of metastatic disease (unsampled) in the left ileum and left femoral shaft.

Special thanks to Dr. Joseph Craig, who provided the radiologic images attached. Also, I wanted to thank Dr. Sean Williamson for providing slides of the open biopsy material.

References:

1. Chen S, Fritchie K, Wei S, Ali N, Curless K, Shen T, Brini AT, Latif F, Sumathi V, Siegal GP, Cheng L. Diagnostic utility of IDH1/2 mutations to distinguish dedifferentiated chondrosarcoma from undifferentiated pleomorphic sarcoma of bone. Hum Pathol. 2017;65:239–46.
2. Kevin, T. Mosaid-pattern dedifferentiation in liposarcoma and chondrosarcoma: imaging features of an uncommon form of dedifferentiation
3. Czerniak, B. editor. Dorfman and Czerniak's Bone Tumors 2nd ed. Philadelphia, PA: Elsevier 2016.